Med. & Biol. Eng. & Comput., 1982, 20, 401–407

Some precautions in the use of time-domain dielectric spectroscopy with biological and other lossy dielectrics

F. X. Hart

Department of Electrical Engineering, The University of Salford, Salford M5 4WT, England

Abstract—*Time-domain dielectric spectroscopy provides a rapid means of obtaining* in vivo *dielectric spectra of biological objects whose physiological state may be changing with time. This paper discusses precautions which must be taken in the selection of the measuring-circuit parameters and frequency range to prevent the introduction of artefacts into the resulting spectra. The ratio of the amplifier input resistance to the sample d.c. resistance should be kept below 0·05. The balancing capacitor should equal as closely as possible the high-frequency capacitance of the sample. The spectrum should be terminated at about 0·7 f* Nyquist.

Keywords—*Biophysical instrumentation, Dielectrics, Impedance*

1 Introduction

MEASUREMENT of the dielectric properties of biological materials has been a topic of considerable interest in recent years. On a fundamental level, the variation of the real and imaginary parts of the relative permittivity with frequency (dielectric spectrum) provides information regarding the electrical structure of the material itself. On an applied level, impedance measurements have been used to monitor physiological states for purposes as diverse as the breeding of cows (EDWARDS, 1980) and the ripening of avocados (BEAN *et al.*, 1960). In such cases, however, little information is available regarding the variation of impedance with frequency. Without knowledge of the full dielectric spectrum, selection of the optimum frequency for characterising a particular physiological state is a matter of chance. Hence, measurement of the full dielectric spectrum of biological materials and its variation with physiological state has important theoretical and practical applications.

The most accurate measurements are made by bridge techniques, which are time consuming especially at very low frequencies. This difficulty is of particular importance for *in vivo* studies of biological materials whose physiological state may be continually changing during the course of the measurement. Time-domain dielectric spectroscopy (t.d.d.s.) provides a rapid, though less accurate, alternative method for obtaining the dielectric spectrum. T.D.D.S. was originally developed for low-loss materials. In particular, HYDE (1970) introduced a system for insulating materials which yielded the relative permittivity and loss factor over the frequency range 10^{-4} to 10^{6} Hz, but which was not very accurate for rather lossy materials. SINGH *et al.* (1979) extended the technique to lossy biological dielectrics. As it can rapidly provide valuable theoretical and practical information on biological systems, it is important that certain precautions in its use, which arise from the lossy nature of the material, be made known.

The author performed this work while on leave from The Department of Physics, The University of the South, Sewanee, TN 37375, USA

First received 14th May and in final form 14th October 1981

0140–0118/82/040401+07$01·50/0

2 Theory

If a constant-voltage pulse V is applied at time $t = 0$ to a lossy dielectric, the resulting current $i(t)$ can be related (SINGH *et al.*, 1979) to both the conductance $G(\omega)$ and capacitance $C(\omega)$ of the sample as a function of the angular frequency $\omega = 2\pi f$ via

$$C(\omega) = C_H + \frac{1}{V}\int_0^\infty i(t)\cos(\omega t)dt \quad . \quad . \quad . \quad (1)$$

and

$$G(\omega) = G_L + \frac{\omega}{V}\int_0^\infty i(t)\sin(\omega t)dt. \quad . \quad . \quad . \quad (2)$$

where G_L and C_H are, respectively, the direct current

conductance and high-frequency capacitance of the sample. Two points must be emphasised:

(*a*) $i(t)$ is the current actually passing through the sample

(*b*) $i(t)$ here does not include the steady-state conduction current.

At low frequencies, most lossy materials exhibit a region of rapid variation of dielectric properties with frequency. The simplest expressions for this alpha dispersion are given by the Debye equations

$$\varepsilon(\omega) = \frac{\varepsilon_L + \varepsilon_H \omega^2 T^2}{1+\omega^2 T^2}$$

$$\sigma(\omega) = \frac{\sigma_L + \sigma_H \omega^2 T^2}{1+\omega^2 T^2}$$

where ε and σ are the permittivity and conductivity of the sample, T is the relaxation time, and the subscripts L and H refer to low- and high-frequency limits. In terms of sample circuit parameters these equations can be rewritten so that

$$C(\omega) = C_H + \frac{(G_H - G_L)\omega^2 T^2}{1+\omega^2 T^2} \quad . \quad . \quad . \quad . (3)$$

and

$$G(\omega) = G_L + \frac{(G_H - C_L)\omega^2 T^2}{1+\omega^2 T^2} \quad . \quad . \quad . \quad . (4)$$

This behaviour can be modelled by two parallel RC combinations connected in series. If R_1, R_2, C_1 and C_2 are the individual elements, then the capacitance of this network is given by eqn. 3, with

$$C_L = (C_1 R_1^2 + C_2 R_2^2)/(R_1 + R_2)^2 \quad . \quad . \quad . (5)$$

$$C_H = C_1 C_2/(C_1 + C_2) \quad . \quad . \quad . \quad . \quad . \quad . (6)$$

and

$$T = R_1 R_2 (C_1 + C_2)/(R_1 + R_2) \quad . \quad . \quad . \quad . (7)$$

The conductance is given by eqn. 4 with

$$G_L = 1/(R_1 + R_2) \quad . \quad . \quad . \quad . \quad . \quad . \quad . (8)$$

and

$$G_H = (R_1 C_1^2 + R_2 C_2^2)/R_1 R_2 (C_1 + C_2)^2 \quad . \quad . (9)$$

In practice, all components of the current-measuring circuit should be included in the analysis lest the measuring process itself introduce artefacts into the results. The following discussion, although it has wider applicability, will be generally based on the t.d.d.s. system originally introduced for biological samples (SINGH *et al.*, 1979).

Fig. 1 illustrates the measuring circuit, in which the sample is depicted as equivalent to the above mentioned RC network. C_0 is a balancing capacitor which will be discussed later. R_a is the input resistance of the operational amplifier circuit used to measure the current. It should be noted that, although the operational amplifier itself has a very high input impedance, R_a is determined primarily by the feedback of this circuit and is much smaller. In fact, the impedance of the current-measuring device must be small in comparison to that of the sample to minimise

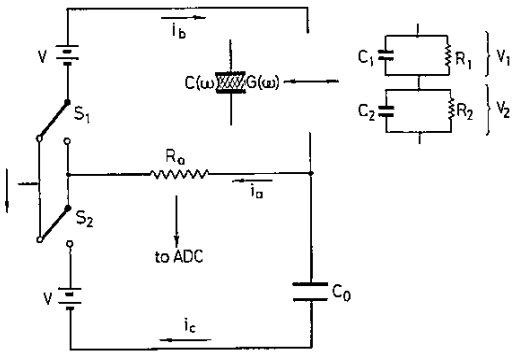

Fig. 1 *T.D.D.S. measuring circuit. C(ω) and G(ω) are the frequency-dependent capacitance and conductance of the sample, which is equivalent to the* RC *network for a Debye response*

error. For low-loss materials, R_a will generally satisfy this condition. However, considerable errors are introduced in the t.d.d.s. of biological and other lossy materials if this precaution is not taken.

Suppose that at $t = 0$ the switches S_1 and S_2 in Fig. 1 are closed simultaneously and voltage pulses are applied to the top and bottom loops of the circuit. Application of Kirchhoff's Laws and the continuity of the total current in the top loop yield

$$i_a = i_b - i_c$$

$$V = q_0/C_0 - i_a R_a$$

$$V = V_1 + V_2 + i_a R_a \quad . \quad . \quad . \quad . \quad . \quad . \quad (10)$$

$$i_b = C_1 \frac{dV_1}{dt} + \frac{V_1}{R_1} = C_2 \frac{dV_2}{dt} + \frac{V_2}{R_2} \quad . \quad . \quad (11)$$

where V_1 and V_2 are the voltage drops across the two RC networks and q_0 is the charge on C_0 at time t.

Use of $i_c = dq_0/dt$ gives

$$i_b = i_a + R_a C_0 \frac{di_a}{dt} \quad . \quad . \quad . \quad . \quad . \quad . \quad (12)$$

Solution of eqns. 10–12 for i_a is not straightforward.

Note, moreover, that the current i_b through the sample is not the same as the current i_a through the measuring device.

An approximate solution can be obtained by recalling that R_a must be small in comparison with the sample resistance. Suppose that C_0 becomes charged through R_a on a time scale $(R_a C_0)$ short in comparison with the relaxation time T of the sample. The bottom loop is, in effect, disconnected from the circuit, and $i_a = i_b$. Eqns. 10 and 11 may be solved with the condition that, at $t = 0$

$$V_1 = V_2 = 0$$

to give

$$i_a = V/R_T + i_1 \exp^{(P_1 t)} + i_2 \exp^{(P_2 t)} \quad . \quad . \quad (13)$$

where

$$R_T = R_1 + R_2 + R_a$$

$$\left.\begin{matrix} P_1 \\ P_2 \end{matrix}\right\} = -(C_1(1+R_a/R_2)+C_2(1+R_a/R_1))$$

$$\pm[(C_1(1+R_a/R_2)+C_2(1+R_a/R_1)^2)^2 - 4R_a C_1 C_2 R_T/R_1 R_2]^{\frac{1}{2}}/2R_a C_1 C_2 \quad . \quad . \quad (14)$$

$$i_1 = (C_1 P_1 + 1/R_1)(R_T + R_a R_1 C_1 P_2)V/R_T R_a C_1 (P_1 - P_2) \quad (15)$$

and

$$i_2 = -(C_1 P_2 + 1/R_1)(R_T + R_a R_1 C_1 P_1)V/R_T R_a C_1 (P_1 - P_2) \quad (16)$$

As the measured relaxation times are $-P_1^{-1}$ and $-P_2^{-1}$ it is clear that eqn. 7 is not satisfied and that Fourier transformation of i_a will not yield the proper expressions for $C(\omega)$ and $G(\omega)$, which should be independent of R_a.

But, in the limit $R_a << R_1, R_2$, eqns. 13–16 become

$$T_1 = -P_1^{-1} = R_1 R_2 (C_1 + C_2)/(R_1 + R_2) = T \quad (17)$$

$$T_2 = -P_2^{-1} = R_a C_1 C_2/(C_1 + C_2) = R_a C_H \quad . \quad (18)$$

$$i_1 = \frac{(R_1 C_1 - R_2 C_2)^2 V}{(R_1 + R_2)(C_1 + C_2)^2 R_1 R_2} \quad . \quad . \quad . \quad . \quad (19)$$

and

$$i_2 = V/R_a \quad . \quad . \quad . \quad . \quad . \quad . \quad . \quad . \quad (20)$$

If $R_a << R_1, R_2$, then $T_1 >> T_2$.

Fourier transformation of eqn. 13 with the application of eqns. 17–20 and 5–9 yields

$$\frac{I}{V}\int_0^\infty i_a(t)\cos(\omega t)dt = \frac{(C_L - C_H)}{1+\omega^2 T^2} + \frac{C_H}{1+\omega^2 T_2^2}$$

and

$$\frac{\omega}{V}\int_0^\infty i_a(t)\sin(\omega t)dt = G_L + \frac{(G_H - G_L)\omega^2 T^2}{1+\omega^2 T^2} + \frac{\omega^2 T_2^2}{R_a(1+\omega^2 T_2^2)}$$

It is assumed here that V is terminated at a time well beyond the duration of the dispersion. For values of ω chosen to best display the alpha dispersion $0{\cdot}1 < \omega T < 10$. Hence $\omega T_2 << 1$. Eqns. 3 and 4 then give

$$\frac{1}{V}\int_0^\infty i_a(t)\cos(\omega t)dt = C(\omega) - C_H + C_H = C(\omega) \quad (21)$$

and

$$\frac{\omega}{V}\int_0^\infty i_a(t)\sin(\omega t)dt = G_L + G(\omega) - G_L + \omega^2 R_a C_H^2 = G(\omega) + \omega^2 R_a C_H^2 \quad . \quad . \quad (22)$$

The $+C_H$ term in eqn. 21 and the $\omega^2 R_a C_H^2$ term in eqn. 22 both originate with the i_2 term in eqn. 13. The relative importance of the $\omega^2 R_a C_H^2$ term increases as the amplitude of the alpha-dispersion decreases. The steady-state direct-current term V/R_t in eqn. 13 produces the $+G_L$ term in eqn. 22 but makes no contribution to $C(\omega)$.

The current passing through the sample i_b is illustrated in Fig. 2. The dispersion current, with

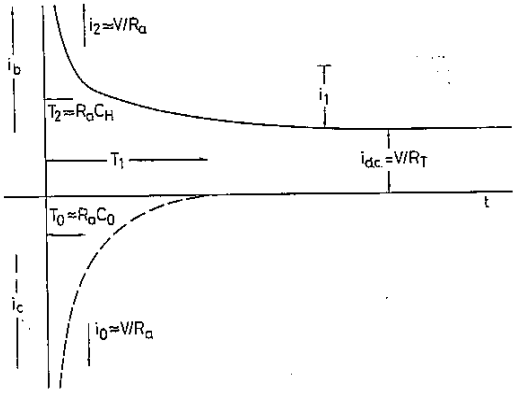

Fig. 2 *Variation of sample current i_b and balancing current i_c with time*

amplitude i_1 and decay time T_1, is preceded by an initial current surge with amplitude i_2 and decay time T_2 and is followed by the steady-state direct current $i_{d.c.}$. As R_a is made smaller, to reduce its contribution to the measured relaxation time, the initial current surge recedes to earlier times but becomes greater in magnitude. For weak alpha dispersion, with i_1 small in comparison with V/R_a, the dispersion current could be easily lost in the tail of the initial current surge, i.e. $\omega^2 R_a C_H^2$ would be comparable with $G(\omega)$.

At this point the bottom loop in the circuit should be recalled. When the switch is closed i_c flows through R_a in a direction opposite to i_b, to charge C_0. This current is illustrated by the broken line in Fig. 2. In particular, if $C_0 = C_H$, the initial current surge through the measuring device should be essentially cancelled. With the i_2 term removed from eqn. 13, the $+C_H$ term in eqn. 21 and the $\omega^2 R_a C_H^2$ term in eqn. 22 disappear to give

$$C(\omega) = C_H + \frac{1}{V}\int_0^\infty I_a(t)\cos(\omega t)dt \quad . \quad . \quad (23)$$

and

$$G(\omega) = \frac{\omega}{V}\int_0^\infty I_a(t)\sin(\omega t)dt \quad . \quad . \quad . \quad . \quad (24)$$

where

$$I_a = i_{d.c.} + i_1 \exp^{(P_1 t)} \quad . \quad . \quad . \quad . \quad . \quad . \quad (25)$$

is the current now passing through the measuring device with the bottom loop introduced to the circuit.

For lossy, biological dielectrics $i_{d.c.}$ can be several times larger than the dispersion current i_1. Considerable error could thus be introduced into the numerical evaluation of the integrals in eqns. 23 and 24 for low frequencies. This difficulty is minimised by subtracting the steady-state current from the measured current before the integration is performed. As $C(\omega)$ does not depend on $i_{d.c.}$, it need be restored only for the evaluation of $G(\omega)$. The equations actually used in the transformation are then

$$C(\omega) = C_H + K\int_0^{T_{max}} (I_a - i_{d.c.})\cos(\omega t)dt \quad . \quad (26)$$

and

$$G(\omega) = Ki_{d.c.} + \omega\Gamma(\omega) \quad . \quad . \quad . \quad . \quad . \quad . \quad (27)$$

where

$$\Gamma(\omega) = K\int_0^{T_{max}} (I_a - i_{d.c.})\sin(\omega t)dt \quad . \quad . \quad (28)$$

$\Gamma(\omega)$, the dielectric loss associated with the dispersion, provides a most sensitive measure of the dispersion process. T_{max} is the time at which the final reading is taken. The lowest frequency obtainable from the transformation is $f_{min} = 1/T_{max}$. From Nyquist's theorem the maximum obtainable frequency is $f_{max} = 1/2T_{min}$, where T_{min} is the time interval between current readings. K is a constant which includes the applied voltage and the proportionality

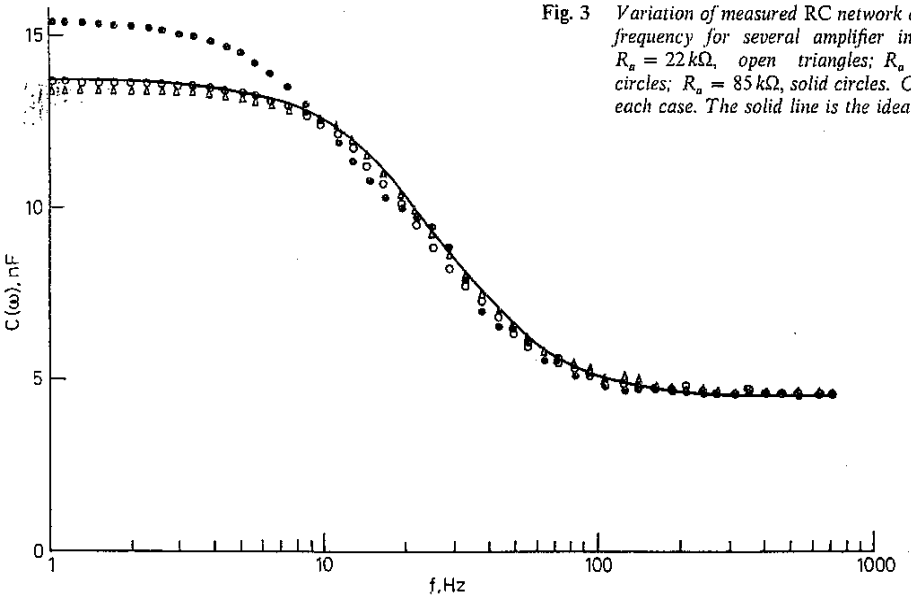

Fig. 3 *Variation of measured* RC *network capacitance with frequency for several amplifier input resistances.* $R_a = 22\,k\Omega$, *open triangles;* $R_a = 56\,k\Omega$, *open circles;* $R_a = 85\,k\Omega$, *solid circles.* $C_0 = 0{\cdot}005\,\mu F$ *in each case. The solid line is the ideal curve*

factors in the amplification and digitisation procedures. K is evaluated by measuring either $G(\omega)$ or $C(\omega)$ or $\Gamma(\omega)$ at any one frequency.

The dielectric loss may be expressed in terms of the sample circuit parameters as

$$\Gamma(\omega) = \frac{(G_H - G_L)\omega T^2}{1+\omega^2 T^2} \quad . \quad . \quad . \quad . \quad . \quad (29)$$

where T, G_L and G_H are given by eqns. 7 to 9, respectively.

3 Results and discussion

Figs. 3 and 4 illustrate the dependence of the capacitance and dielectric loss spectra on the choice of amplifier input resistance. The theoretical spectra calculated from eqns. 3 to 9 and 29 for $R_1 = R_2 = 220\,k\Omega$, $C_1 = 0{\cdot}05\,\mu F$ and $C_2 = 0{\cdot}005\,\mu F$ are plotted as solid lines. The experimental points are obtained by Fourier transformation of the current measured by the circuit illustrated in Fig. 1, using eqns. 26 and 28, with the above values for R_1, R_2, C_1 and C_2 and with $C_0 = 0{\cdot}005\,\mu F$. K is evaluated by equating the theoretical and experimental dielectric losses at 25 Hz. With the capacitance spectrum good agreement is obtained between the theoretical curve and the experimental values for $R_a = 19{\cdot}5$ and $56\,k\Omega$, but serious divergence appears at low frequencies for $R_a = 85\,k\Omega$. The experimental dielectric-loss spectra agree well with the theoretical curve for the two lowest R_a values, although a slight shift of the peak to lower frequencies is detectable for $R_a = 56\,k\Omega$. The experimental spectrum for $R_a = 85\,k\Omega$ is, however, seriously distorted by the presence of two peaks. Since the total 'sample' resistance is $440\,k\Omega$, it is clear that minor differences appear in the spectra at $R_a/R_{sample} = 0{\cdot}11$, and serious distortions occur at $R_a/R_{sample} = 0{\cdot}19$. Furthermore, the distortion is not simply a broadening of the peak but a change in the overall shape of the curve.

The distortions produced by large R_a values can be understood in the following way. The measured current has two characteristic decay times, $T_1 = -P_1^{-1}$ and $T_2 = -P_2^{-1}$, as well as a single balancing risetime, $T_0 = R_a C_0$. Fourier transformation leads to two loss peaks at $f_1 = (2\pi T_1)^{-1}$ and $f_2 = (2\pi T_2)^{-1}$, in addition to a loss 'well' at $f_0 = (2\pi T_0)^{-1}$. For $C_0 \approx C_H$ the well at f_0 tends to cancel the peak at f_2. For $R_a << R_1, R_2$, any imbalance is displaced to times considerably before the first measuring interval. But, for larger values of R_a, any imbalance appears as a distortion in the capacitance spectrum and, more noticeably, in the loss spectrum. With $R_1 = R_2 = 220\,k\Omega$, $C_1 = 0{\cdot}5\,\mu F$ and $C_0 = C_2 = 0{\cdot}005\,\mu F$, eqn. 14 yields:

(*a*) for $R_a = 19{\cdot}5\,k\Omega$, $f_1 = 25{\cdot}6$ Hz, $f_2 = 1930$ Hz and $f_0 = 1620$ Hz

(*b*) for $R_a = 56\,k\Omega$, $f = 24{\cdot}6$ Hz, $f_2 = 830$ Hz and $f_0 = 640$ Hz

(*c*) for $R_a = 85\,k\Omega$, $f_1 = 23{\cdot}6$ Hz, $f_2 = 540$ Hz and $f_0 = 390$ Hz.

Although the position of the dispersion loss peak f_1 is not strongly dependent on R_a, both the f_2 peak and the f_0 well are shifted into the dispersion region. Furthermore, since the initial surge and balancing currents are considerably larger than the dispersion current, any imbalance in their tails then causes significant distortion of the transformed spectra. A more thorough analysis would require the simultaneous numerical solution of eqns. 10 to 12.

Figs. 5 and 6 illustrate the dependence of the capacitance and dielectric loss spectra on the choice of balancing capacitor C_0. The theoretical spectra are again plotted as solid lines.

$R_a = 56\,k\Omega$ for the three experimental spectra corresponding with $C_0 = 0{\cdot}002$, $0{\cdot}005$ and $0{\cdot}010\,\mu F$. For comparison, $C_H = 0{\cdot}0045\,\mu F$. Significant errors in the low-frequency capacitance and the presence of double peaks in the loss spectrum indicate the existence of an imbalance of the initial surge and balancing currents for the $0{\cdot}002$ and $0{\cdot}010\,\mu F$ cases. The greater distortions produced by the former

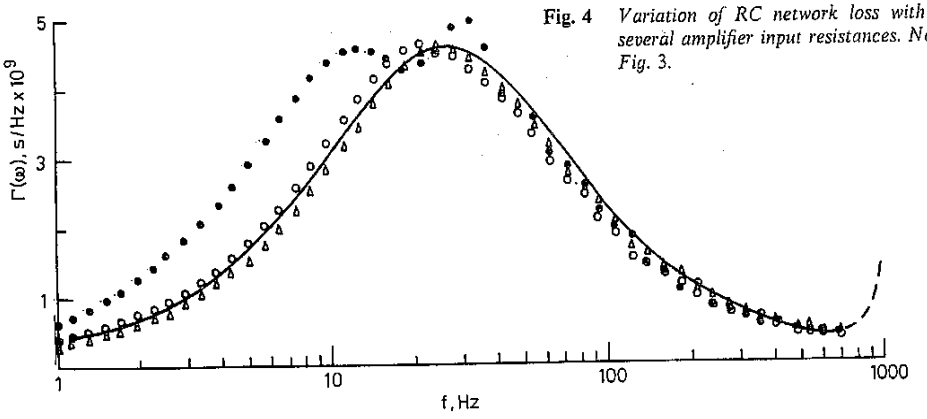

Fig. 4 *Variation of RC network loss with frequency for several amplifier input resistances. Notation is as in Fig. 3.*

indicate that it would be better to select a value for C_0 which is too high rather than one which is too low.

For $R_a = 19{\cdot}5\,k\Omega$, no significant differences could be observed in the spectra produced with these three values of C_0.

The need for precautions in the production and interpretation of dielectric spectra generated in the time domain should now be apparent. The lower loop in the measuring circuit provides a balancing current to cancel the initial current surge through the measuring device. R_a must be small in comparison with the sample resistance to displace any imbalance in the tails of these currents to times well before the first measuring interval. In practice, the d.c. resistance of the sample should first be measured and the input resistance of the amplifier circuit adjusted, by the introduction of a shunt if necessary, so that $R_a/R_{sample} < 0{\cdot}05$. Because R_a depends upon the details of the amplifier circuit (e.g. the gain) its values should be measured.

Although the exact matching of C_0 and C_H is not critical for small R_a, large differences must be avoided. For $R_a/R_{sample} > 0{\cdot}01$, a small mismatch can lead to serious errors in the spectra. This matching can be achieved in two ways. The sample capacitance could be measured at one frequency, well above the dispersion, to yield C_H. Alternatively, the output from the amplifier circuit could be monitored by a storage oscilloscope and C_0 adjusted to eliminate any tails due to the imbalance of the initial surge and balancing currents. It is not sufficient that the output simply be positive at the first measuring interval. This was the

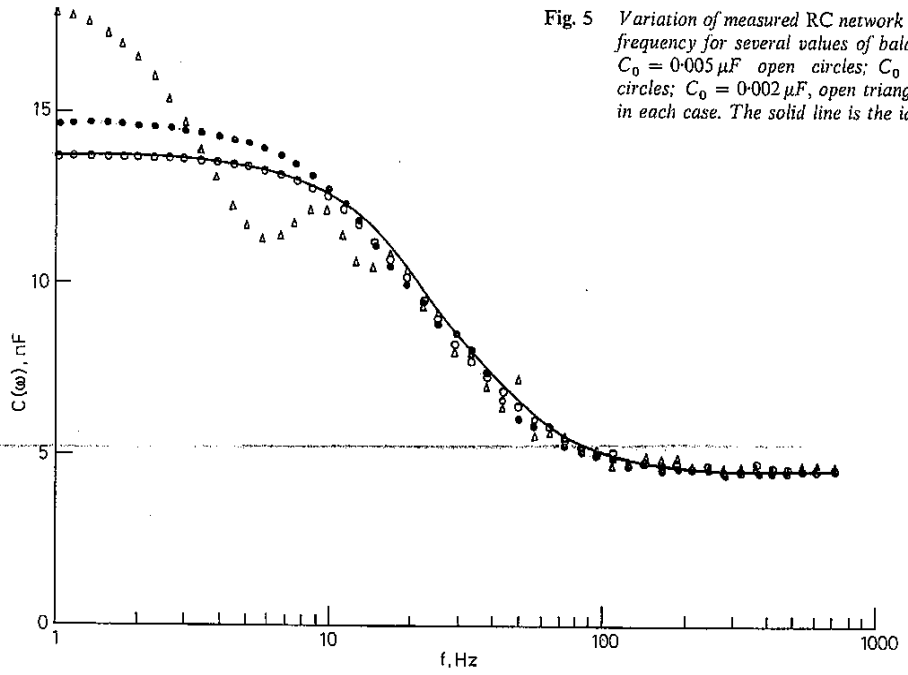

Fig. 5 *Variation of measured* RC *network capacitance with frequency for several values of balancing capacitor. $C_0 = 0{\cdot}005\,\mu F$ open circles; $C_0 = 0{\cdot}01\,\mu F$ solid circles; $C_0 = 0{\cdot}002\,\mu F$, open triangles. $R_a = 56\,k\Omega$ in each case. The solid line is the ideal curve*

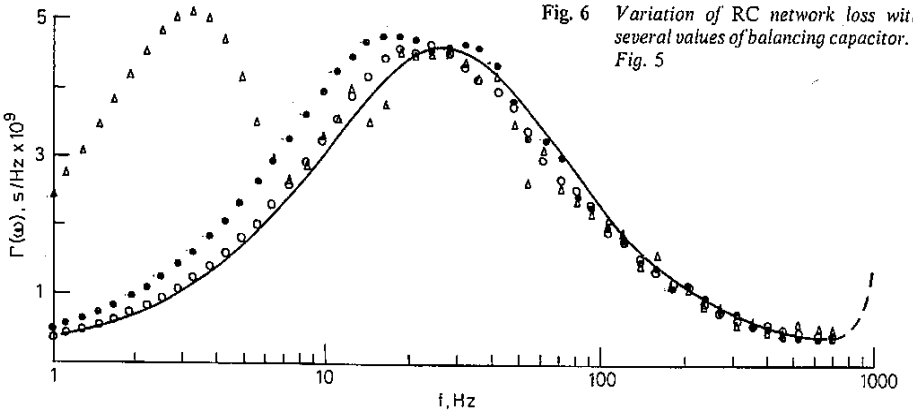

Fig. 6 *Variation of* RC *network loss with frequency for several values of balancing capacitor. Notation is as in Fig. 5*

case for all three experimental curves in Figs. 5 and 6. If in doubt, it is better to err on the high side in selecting C_0.

It should also be noted that the addition of the lower loop with C_0 in no way protects the sample from the large, though short-lived, initial current surge. The current passing through the sample is given by eqn. 13. The lower loop eliminates the current surge from the measuring device, not the sample. If the current through the sample must be limited to minimise electrode effects or tissue damage, use of a current-limiting resistance in series with the sample will distort the spectrum and must be avoided. A smaller voltage pulse must be applied instead and greater amplification used.

One further precaution should be noted. Even for $f < f_{max}$, errors can be introduced into the spectra by the numerical procedures used to evaluate the integrals in eqns. 26–28. With a measuring interval of 0·5 ms, $f_{max} = 1000$ Hz. In evaluating these expressions for $f = 667$ Hz only three discrete values of the integrand are present per cycle; at higher frequencies, even fewer. Furthermore, if $f_1 << f_{max}$, the dispersion current varies relatively slowly during the first few measuring intervals, and the integrands oscillate very rapidly with a slowly decreasing amplitude. The relative paucity of points combined with the rapidity of oscillation severely reduces the accuracy of the numerical integration and may even introduce spurious structure, which depends on the particular choice of numerical method, into the spectra.

Such frequency 'aliasing' can be demonstrated by calculating a 'theoretical' current with eqn. 25 and integrating it numerically with the use of eqn. 28 and Simpson's Rule.

For $R_1 = R_2 = 220\,\text{k}\Omega$, $C_1 = 0{\cdot}05\,\mu\text{F}$ and $T_{min} = 0{\cdot}5$ ms the resulting loss curve is identical with the ideal loss curve in Figs. 4 and 6 up to about 650 Hz. At higher frequencies a spurious loss peak, represented by the broken line in those diagrams, appears. Use of the trapezoidal rule led, instead, to a spurious decease at those higher frequencies.

If f_1 is closer to f_{max}, the dispersion current decreases more rapidly in the first few intervals, the oscillations in the integrand are more rapidly damped out, and the inaccuracies become less important. Care should then be taken in the interpretation of the shapes of the spectra at high frequencies, even below f_{max}.

4 Conclusions

The double-loop t.d.d.s. circuit can provide a rapid means for measuring the dielectric spectrum of biological and other lossy materials. Serious errors will enter, however, unless precautions are taken to ensure that $R_a << R_{sample}$ and $C_0 = C_H$, and to terminate the spectrum well below f_{max}. Failure to do so will lead to spurious structure in the spectra which could confuse the interpretation of the results.

Acknowledgment—I would like to express my appreciation to Dr. C. W. Smith for helpful discussions on this subject.

References

BEAN, R. C., RASOR, J. P. and PORTER, G. C. (1960) Changes in the electrical characteristics of avocados during ripening. *Yearb. Calif. Avocado Soc.*, **44**, 75–78.

EDWARDS, D. F. (1980) Proposed instrumentation to determine the optimum time to inseminate cattle by measurement of vaginal impedance. *Med. & Biol. Eng. & Comput.*, **18**, 73–80.

HYDE, P. J. (1970) Wide-frequency-range dielectric spectrometer. *Proc. IEE*, **117**, (9) 1891–1901.

SINGH, B., SMITH, C. W. and HUGHES, R. (1979) *In vivo* dielectric spectrometer. *Med. & Biol. Eng. & Comput.*, **17**, 45–60.